sciendo

ARTIFICIAL SATELLITES, Vol. 56, No. 2 – 2021
DOI: 10.2478/arsa-2021-0003

PERFORMANCE ASSESSMENT OF PPP-AR POSITIONING AND ZENITH TOTAL DELAY ESTIMATION WITH MODERNIZED CSRS-PPP

Omer Faruk ATIZ, Ibrahim KALAYCI

Department of Geomatics Engineering, Necmettin Erbakan University, Konya, Turkey

e-mails: oatiz@erbakan.edu.tr, ikalayci@erbakan.edu.tr

ABSTRACT. The precise point positioning (PPP) method has become more popular due to powerful online global navigation satellite system (GNSS) data processing services, such as the Canadian Spatial Reference System-PPP (CSRS-PPP). At the end of 2020, the CSRS-PPP service launched the ambiguity resolution (AR) feature for global positioning system (GPS) satellites. More reliable results are obtained with AR compared to the results with traditional ambiguity-float PPP. In this study, the performance of the modernized CSRS-PPP was comparatively assessed in terms of static positioning and zenith total delay (ZTD) estimation. Data for 1 month in the year 2019 obtained from 47 international GNSS service (IGS) stations were processed before and after modernization of the CSRS-PPP. The processes were conducted for GPS and GPS + GLONASS (GLObalnaya NAvigatsionnaya Sputnikovaya Sistema) satellite combinations. Besides, the results were analyzed in terms of accuracy and convergence time. According to the solutions, the AR feature of the CSRS-PPP improved the accuracy by about 50% in the east component for GPS + GLONASS configuration. The root-mean-square error (RMSE) of the ZTD difference between modernized CSRS-PPP service and IGS final troposphere product is 5.8 mm for the GPS-only case.

Keywords: ambiguity resolution, CSRS-PPP, precise point positioning, zenith total delay

1. INTRODUCTION

Precise point positioning (PPP) is a powerful positioning technique that can provide millimeter-to-centimeter level of accuracy after a convergence time using precise satellite orbit, clock, and other related products (Earth rotation parameter, differential code bias, and so on) (Kouba and Héroux 2001; Zumberge et al., 1997). In the past years, the PPP method has been extensively used in different studies for applications, such as determining displacements, surface deformation, landslide monitoring, aircraft positioning, or even in smartphones (Alcay et al., 2019; Atiz et al., 2020; Goudarzi and Banville, 2018; Krasuski et al., 2018; Wang et al., 2015; Wu et al., 2019; Yigit et al., 2014). The global navigation satellite system (GNSS) is used to determine the position, time, and navigation, as well as estimate the total electron content (TEC) in the ionosphere layer (Otsuka et al., 2002) and zenith total delay (ZTD) in the troposphere (Pikridas et al., 2014). However, for PPP postprocessing, many software packages have been developed, e.g., RTKLIB (Real-Time Kinematic Library) (Takasu and Yasuda, 2009), GipsyX (Bertiger et al., 2020), and PRIDE

PPP-ambiguity resolution (AR) (Geng et al., 2019). In addition, some online software [e.g., Canadian Spatial Reference System-PPP (CSRS-PPP)] provide free PPP processing service for only users registering with a valid mail address. The PPP method has become more popular with free and user-friendly software, such as MG-APP (multi-GNSS automatic precise positioning software) (Xiao et al., 2020), and online services that do not require any expertise in the GNSS data-processing field, with the advantage of reduced field cost.

The CSRS-PPP service is an online PPP postprocessing service developed in 2003 and operated by Natural Resources Canada (NRCan) to date (Tétreault et al., 2005). There are many studies on the performance of CSRS-PPP and other online GNSS data-processing services. Guo (2015) compared the precisions of the automatic precise positioning service (APPS), GPS analysis and positioning software (GAPS), CSRS-PPP, and Magic-PPP software in terms of static positioning and ZTD estimation. The results indicated that all four software can give millimeter-to-centimeter level positioning accuracy. The results also indicated that the accuracy of ZTD estimation derived from these online GNSS data-processing services is on the scale of a few centimeters. Mendez Astudillo et al. (2018) compared three online (CSRS-PPP, APPS, and Magic-PPP) and three offline (POINT, RTKLIB, and GNSS Lab Tool suite-GLAB) PPP software in terms of ZTD estimation. It was demonstrated that ZTD estimation of CSRS-PPP is very accurate. The root-mean-square errors (RMSEs) of the difference from international GNSS service (IGS) final troposphere products are mostly <1.0 cm. Bulbul et al. (2021) investigate the performances of CSRS-PPP, Magic-GNSS, and APPS online services, at regions with different urban densities. They demonstrated that the accuracy of CSRS-PPP is better than that of other services for all the tested 1-, 2-, 4-, and 6-hour sessions. In general, CSRS-PPP service is more reliable than other online PPP services from both positioning and troposphere estimation aspects.

Apart from the postprocessing, the PPP method can be used in real time due to the availability of IGS real-time precise products (Krzan and Przestrzelski, 2016). Nevertheless, the real-time PPP method is not convenient for high-accuracy applications due to the low accuracy of real-time orbit and clock products (Alcay and Turgut, 2021; Elsobeiey and Al-Harbi, 2016).

In the traditional PPP approach (Zumberge et al., 1997), the phase ambiguities are not fixed to integer values and remain real-valued. The accuracy of the solution is degraded since the ambiguity parameter is still real-valued after the convergence time (Shi, 2012). The hardware biases arising from both satellites and receivers need to be eliminated for PPP with AR (Ogutcu, 2020a). The IGS analysis centers – e.g., Center for Orbit Determination in Europe, Centre National d'Études Spatiales (CNES), NRCan, and Wuhan University – produce additional phase/clock bias information from a network (Banville et al., 2020). On the other hand, due to different PPP-AR strategies, the analysis centers use different methods to calculate biases. Therefore, the usage of phase/clock bias products can only be possible with suitable software. Many studies have been conducted using the PPP-AR method (Goudarzi and Banville, 2018; Hu et al., 2014; Katsigianni et al., 2019; Li et al., 2018; Tegedor et al., 2015). Hu et al. (2014) have investigated the performance of PPP-AR in a mining field with their proposed zero-differenced ambiguity-fixing model. The results showed that PPP-AR improved the 3D-positioning accuracy by >70%. In Katsigianni et al. (2019), the performances of the kinematic postprocessed PPP and the PPP-AR methods were analyzed. For GPS-only kinematic PPP-AR, accuracy levels of 9.3/8.3 mm and 24.0 mm were obtained for the horizontal components and the vertical component, respectively. AR improved the PPP solutions by 1–3 mm for the east and north components. Tegedor et al. (2015) compared the Real Time Kinematic (RTK), PPP, and PPP-AR methods in a vessel moving through Oslo, Norway. The phase bias information for PPP-AR was generated from two different nearby stations. The results showed that the AR approach on PPP improved the positioning

accuracy. Goudarzi and Banville (2018) evaluated the performance of the static relative and static PPP-AR approaches for determining land surface deformations. It was concluded that the PPP-AR method showed better accuracy in terms of positioning and velocity. The results also indicated that the PPP-AR processing time is significantly lower than that for the relative method. Li et al. (2018) developed a multi-GNSS phase bias estimation model and multi-GNSS PPP-AR positioning model. According to their results, for 2-hour sessions, the GPS-only PPP-AR provided an accuracy level of 0.6/0.5/1.9 cm for the north, east, and up components, respectively.

Moreover, the CSRS-PPP announced a modernization related to the software engine in 2018. This modernization, which includes GPS AR, has become publicly available at the end of 2020. For more detailed information about the changes in the software, the reader is referred to Banville (2020).

This study aims to investigate the performance of the modernized CSRS-PPP service in terms of static positioning and ZTD estimation. For this purpose, 31 consecutive daily data of 47 IGS stations in 2019 were processed before and after the modernization of the software. The processes were performed not only using GPS satellites but also combined with GLONASS because the benefits of the combined use of different GNSSs are explicit, particularly under limited sky view conditions (Alcay and Yigit, 2017; Alcay et al., 2012; Cai et al., 2013; Jokinen et al., 2013; Ogutcu, 2020b; Ogutcu and Kalayci, 2016). Consequently, four different solutions for each observation were obtained with GPS and GPS + GLO combinations, in two steps, namely, PPP and PPP-AR. The position and ZTD results were evaluated in comparison to IGS weekly solutions and IGS final troposphere product, respectively.

2. PPP WITH AR

In GNSS data processing, linear combinations of observations are used in many cases instead of raw observations, e.g., the first-order effect of the ionosphere can be removed using the iono-free (IF) combination (Subirana et al., 2013). In the traditional PPP model, AR is not implemented due to the biases originating from GNSS hardware. In addition to precise satellite orbit and clock correction, IGS analysis centers also calculate the satellite phase bias information, which is necessary to acquire an ambiguity-fixed PPP solution (Håkansson et al., 2017). For ambiguity-fixed PPP with IF combination, several approaches have been developed, such as the integer recovery clock (IRC) model (Laurichesse et al., 2009), the decoupled satellite clock (DSC) model (Collins et al., 2010), and the uncalibrated phase delay (UPD) model (Ge et al., 2008). The same approach used by the analysis center for producing phase/clock bias information should be applied to user solutions. Here, the utilization of phase/clock bias products is software dependent. The CSRS-PPP with AR is based on the DSC model. Therefore, the functional model of the DSC model is briefly introduced below.

The IF code and phase observables between a receiver–satellite pair can be written as follows (Leick et al., 2015):

$$P_{IF} = \rho + c \cdot (dt^r - dt^s) + d_{trop} + b^r_{P,IF} - b^s_{P,IF} + \epsilon_{P,IF}, \quad (1)$$

$$\emptyset_{IF} = \rho + c \cdot (dt^r - dt^s) + d_{trop} - \lambda_{IF} \cdot N_{IF} + b^r_{\emptyset,IF} - b^s_{\emptyset,IF} + \epsilon_{\emptyset,IF}, \quad (2)$$

where P_{IF} and $\emptyset_{IF}$ represent the IF code and phase observables, respectively; superscript r and s indicate the receiver and the satellite, respectively; ρ is the geometric distance between the receiver and the satellite; c is the speed of light; dt^r is the receiver clock error; dt^s is the satellite clock error; $b^r_{P,IF}$ and $b^s_{P,IF}$ are the IF code biases for the receiver and the satellite, respectively; $b^r_{\emptyset,IF}$ and $b^s_{\emptyset,IF}$ are the IF phase biases for the receiver and the satellite,

respectively; λ_{IF} is the IF wavelength; N_{IF} is the real-valued IF ambiguity term; and $\epsilon_{P,IF}$ and $\epsilon_{\emptyset,IF}$ are the code and phase measurement noises, respectively.

For the sake of simplicity, the common errors that are appropriately modeled or eliminated, such as satellite orbit error, phase wind-up, receiver/satellite antenna phase center variations, and relativistic effects, are not given in Eqs. (1) and (2). The ambiguity term in traditional PPP is real-valued as it absorbs the receiver and satellite code/phase biases. Therefore, additional phase/clock biases are necessary for integer ambiguity-resolved PPP. However, the ambiguity-fixed solution is only attainable when the receiver and the satellite code/phase biases are calibrated.

The DSC model introduced by Collins et al. (2010) includes another linear combination named Melbourne–Wübbena (MW) besides the IF combinations (Melbourne, 1985; Wübbena, 1985). The MW combination is the difference between wide-lane (WL) phase and narrow-lane (NL) code observations. The wavelengths of WL and NL combinations can be written as follows:

$$\lambda_{WL} = \frac{c}{f_1 - f_2};\ \lambda_{NL} = \frac{c}{f_1 + f_2}, \tag{3}$$

where λ_{WL} represents the WL wavelength, λ_{NL} is the NL wavelength, f_1 and f_2 are the dual frequencies (e.g., GPS L1: 1575.42 MHz and L2: 1227.60 MHz). Accordingly, the MW observable is expressed as follows:

$$MW = -\lambda_{WL} \cdot N_{WL} + b^r_{MW} - b^s_{MW} + \epsilon_{MW}, \tag{4}$$

where N_{WL} represents the WL ambiguity, b^r_{MW} and b^s_{MW} are the MW receiver and satellite biases, and ϵ_{MW} is the unmodeled error of MW combination. The PPP DSC model consists of three observables, as shown in Eqs. (1), (2), and (4). The unknown parameters of the DSC model are as follows:

$$X = \left[\bar{x}, d_{trop}, dt^r, dt^s, b^r_*, b^s_*, \widetilde{N_{WL}}, \widetilde{N_{IF}}\right], \tag{5}$$

where $\bar{x}$ is the receiver position update vector; b^r_* and b^s_* are the observation-specific receiver and satellite phase/code biases; and $\widetilde{N_{WL}}$ and $\widetilde{N_{IF}}$ are the WL and IF ambiguities for each satellite. Because the number of unknown parameters is more than the number of observations, a datum deficiency problem occurs. To resolve this issue, a two-step approach is used, namely, parameter reconstruction and introducing two new datums. First, the IF ambiguity in Eq. (2) is decomposed as follows:

$$\lambda_{IF} \cdot N_{IF} = \lambda_{IF} \cdot (17N_1 + 60N_{WL}), \tag{6}$$

where N_1 is the carrier phase ambiguity on f_1 frequency. Moreover, the decoupled clocks are obtained with the combination of the clock parameters and their code/phase bias counterparts. For instance, the decoupled code clock for a receiver is equal to $dt^r + b^r_{P,IF}$. Consequently, the observation equations for the reconstructed DSC model is formed as follows:

$$\begin{aligned} P_{IF} &= \rho + c \cdot \left(dt^r_{P,IF} - dt^s_{P,IF}\right) + d_{trop} + \epsilon_{P,IF} \\ \emptyset_{IF} &= \rho + c \cdot \left(dt^r_{\emptyset,IF} - dt^s_{\emptyset,IF}\right) + d_{trop} - \lambda_{IF} \cdot (17N_1 + 60N_{WL}) + \epsilon_{\emptyset,IF}, \\ MW &= \left(b^r_{MW} - b^s_{MW}\right) - \lambda_{WL} \cdot N_{WL} + \epsilon_{MW} \end{aligned} \tag{7}$$

where $dt^r_{P,IF}$ and $dt^s_{P,IF}$ indicate the code-decoupled receiver and satellite clocks, and $dt^r_{\emptyset,IF}$ and $dt^s_{\emptyset,IF}$ indicate the phase counterparts. The second step includes the definition of two new datums, namely, clock datum and ambiguity datum (Shi and Gao, 2014). The clock datum is determined as follows: first, a reference receiver is selected, and then its code/phase biases are

nullified. The ambiguity datum is constructed as determining a reference satellite and appointing its N_1 and N_{WL} ambiguities to random integer numbers. Thus, the datum deficiency problem is clarified. For more information about solving the datum deficiency problem, the reader is referred to Shi (2012). The integer value of the ambiguity term is calculated using these three DSCs.

The above-mentioned functional model can be applied for a single system PPP-AR. However, GPS (AR) + GLONASS (float) solutions were derived in addition to GPS (AR). The combined GPS + GLONASS PPP model is not given considering the scope of this study. The reader is referred to Cai and Gao (2013) for information about the GPS + GLONASS PPP model.

3. DATA AND PROCESSING STRATEGY

A set of 31-day data from geographically well-distributed 47 IGS stations in 2019 was processed to test the performance of the modernized CSRS-PPP with AR. The data availability was checked on the epoch basis using in-house software. Then, only the observation files that have >90% available data were used in the processes. The processes were performed for both GPS-only and GPS + GLO satellite configurations. Therefore, the IGS stations were selected considering GLONASS availability. To validate the positioning accuracy, IGS weekly combined solutions were taken as the reference coordinates. The locations of the selected IGS stations are depicted in Figure 1.

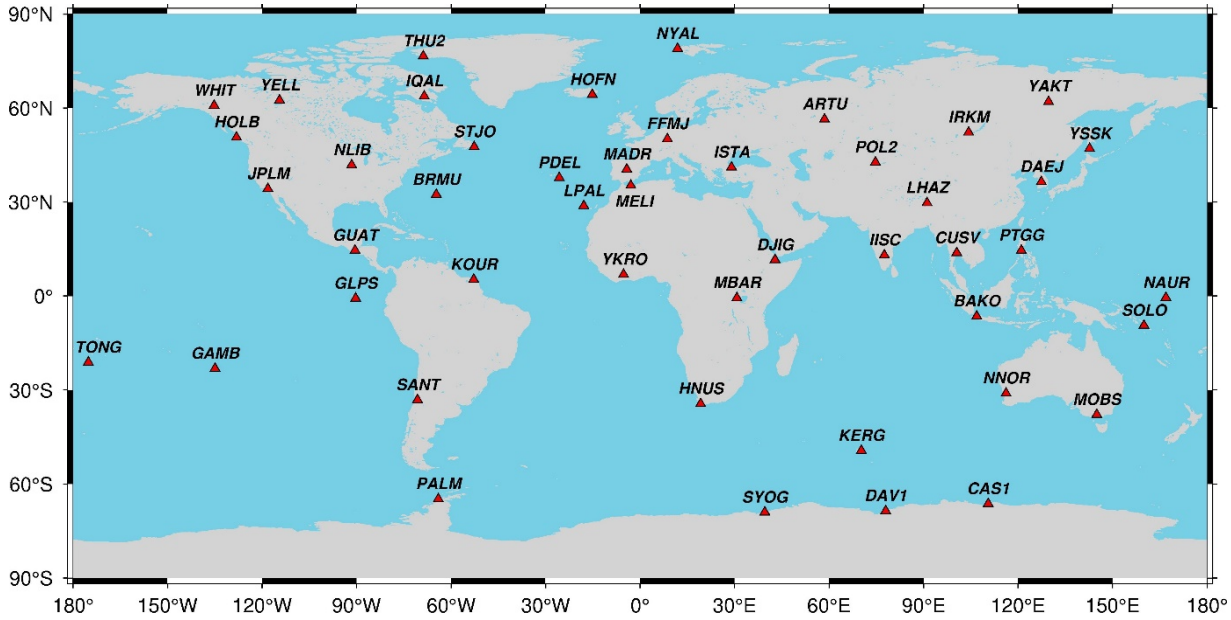

Figure 1. The location of selected IGS stations

The static PPP solutions were computed in two steps: before the software transition to AR, and, after the modernization. Thus, PPP and PPP-AR solutions were obtained for GPS and GPS + GLO satellite configurations. The data-processing strategy for both solutions is provided in Table 1.

Table 1. Data processing strategy

Parameter	PPP	PPP-AR
GNSS	GPS/GPS+GLO	GPS/GPS+GLO
CSRS-PPP version	2.31.0	3.45.0
Processing mode	Static	Static
Filtering	Forward	Forward
Epoch interval	30 s	30 s
Cut-off angle	7.5°	7.5°
Observations	Phase and code	Phase and code
Frequencies	GPS: C1W, C2W, L1W, L2W GLO: C1P, C2P, L1P, L2P	GPS: C1W, C2W, L1W, L2W GLO: C1P, C2P, L1P, L2P
Satellite orbit and clock	IGS Final	NRCan Final
Satellite phase ambiguity bias	N/A	NRCan
Ambiguities	Float	Fixed by using DSC model
Ambiguity validation	N/A	Weighted Integer Decision (Banville et al., 2021)
Estimated parameters	Coordinates, Total Zenith Delay, Receiver Clock, Ambiguities, Slant Total Electron Content	Coordinates, Total Zenith Delay, Receiver Clock, Ambiguities, Slant Total Electron Content
Receiver clock	Estimated as white noise	Estimated as white noise
A priori troposphere	Vienna Mapping Function 1 (VMF1) grid files	Vienna Mapping Function 1 (VMF1) grid files
Tropospheric zenith delay	Random walk 5.0e-5 m/sqrt(sec)	Random walk 5.0e-5 m/sqrt(sec)
Troposphere gradients	Random walk 1.667e-6 m/sqrt(sec)	Random walk 1.667e-6 m/sqrt(sec)
Slant ionosphere delay	White noise 0.1 m/sqrt(sec)	White noise 0.1 m/sqrt(sec)
Reference Frame	ITRF 2014	ITRF 2014
Earth rotation parameters	IGS .erp file	NRCan .erp file
Tidal effects	Corrected (IERS Conventions, 2010)	Corrected (IERS Conventions, 2010)
Antenna phase center offsets	Corrected (Up-to-date NRCan IGS14.atx file)	Corrected (Up-to-date NRCan IGS14.atx file)

The cartesian coordinates (X, Y, Z) and ZTDs were obtained after utilizing the processes over e-mail.

Before PPP performance analysis, changes in the ionosphere during the observations were investigated since anomalies in the ionosphere layer can disturb the PPP results. Substantial variations in the TEC value can indicate an ionospheric storm. Moreover, the space weather condition indices provide information about ionospheric anomalies. There is an ionospheric storm when any index value exceeds its expected threshold (Alcay and Gungor, 2020). The geomagnetic storm (Kp), geomagnetic activity (Dst), and solar activity (F10.7) index values (https://omniweb.gsfc.nasa.gov/form/dx1.html) were analyzed to check whether there was any ionospheric storm during the observations (Figure 2).

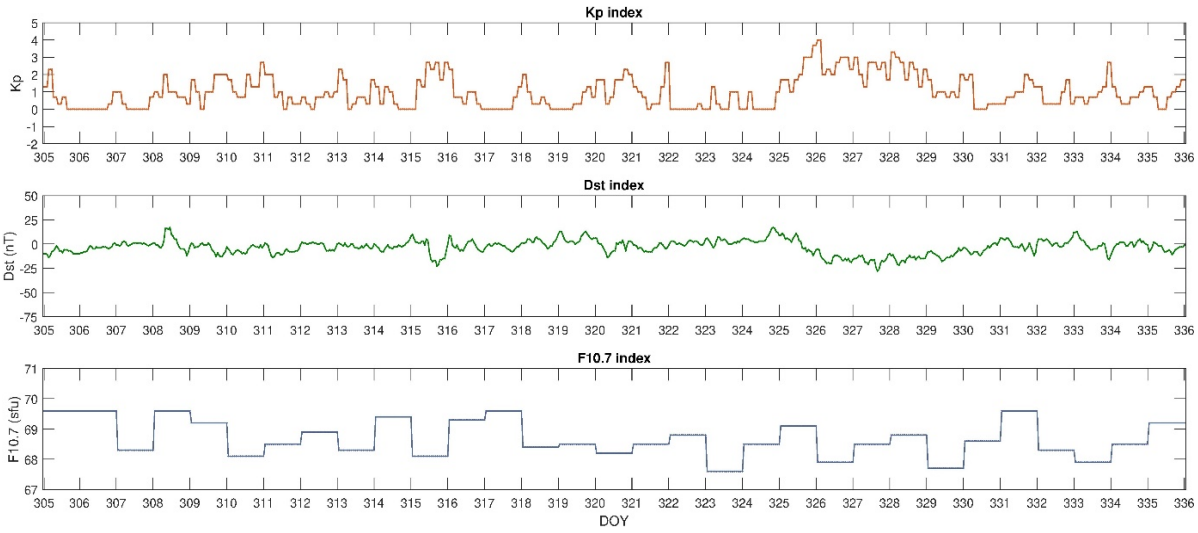

Figure 2. The Kp, Dst, and F10.7 index values

Figure 2 illustrates that there is no global ionosphere-induced storm that could affect the GNSS observations during day of year (DOY) 305–336.

4. POSITIONING AND ZTD RESULTS

The ambiguity-fixing rates were computed as they are crucial for PPP-AR processing. Herein, the fix rate is the percentage of resolved carrier phase ambiguities out of the total phase measurements (Banville et al., 2021). It should also be noted that only GPS ambiguities are fixed in the current PPP model of CSRS-PPP. Regarding the results, at least 84.40% and 79.75% of the ambiguities were fixed for GPS and GPS + GLO satellite combinations, respectively. When the average ambiguity-fixing rates were examined, 97.62% and 97.68% of ambiguities were resolved for GPS and GPS + GLO satellite combinations, respectively. According to these results, the modernized CSRS-PPP software has successfully applied the PPP-AR method.

The obtained Cartesian coordinates were converted to the topocentric system (north, east, up) with respect to IGS weekly combined solutions. Then, the RMSE values for the results of each station were calculated. Only the overall RMSEs are presented in this manuscript for the sake of simplicity. Table 2 gives the overall RMSEs computed with GPS and GPS + GLO satellite configurations for PPP and PPP-AR solutions.

Table 2. RMS errors for GPS solutions

GPS		
	PPP	**PPP-AR**
North (mm)	1.84	1.68
East (mm)	2.61	1.41
Up (mm)	5.21	4.58
GPS+GLO		
	PPP	**PPP-AR**
North (mm)	1.81	1.67
East (mm)	2.69	1.38
Up (mm)	4.92	4.59

Table 2 displays that the GPS-only PPP offers accuracy of 1.84 mm, 2.61 mm, and 5.21 mm for the north, east, and up components, respectively. When the PPP-AR counterparts are considered, AR visibly improves the results, particularly in the east component. The improvement percentages are illustrated in Figure 3 to visualize the accuracy improvement of PPP-AR compared to PPP.

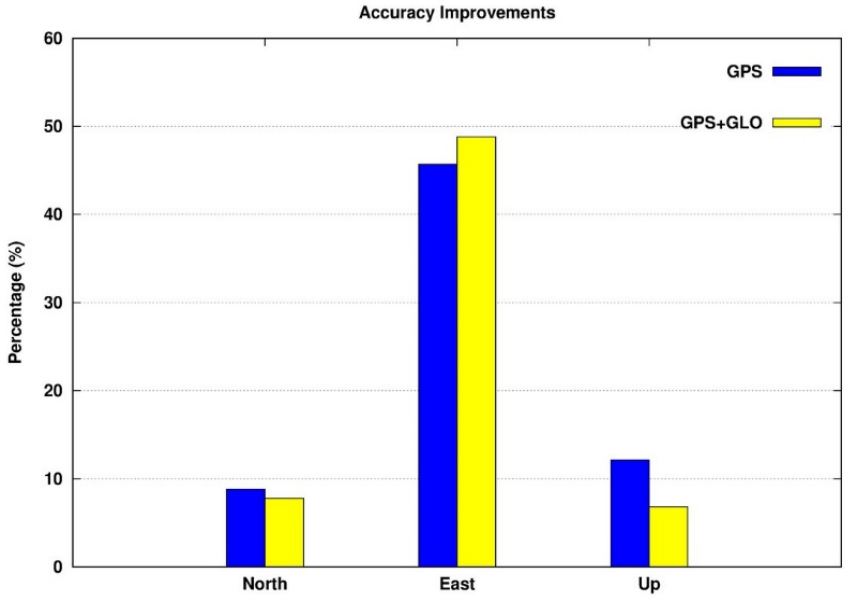

Figure 3. The improvements in accuracy on using the AR approach

As shown in Figure 3, the AR approach improved solutions in the north and up components by about 10%. AR significantly contributed to the east component with almost 50%. However, Figure 3 implies that the difference between GPS and GPS + GLO satellite combinations is not significant in terms of overall accuracy. Bertiger et al. (2020) investigate the static PPP performance of Jet Propulsion Laboratory's (JPL) GipsyX software, using 24-hour data sets. They reported that GipsyX provides an accuracy of 1.90 mm, 1.98 mm, and 6.47 mm for the north, east, and up components, respectively. When compared to the experimental results of this study, the modernized CSRS-PPP software offered slightly better results than GipsyX for both horizontal and vertical components.

The repeatability of solutions should be analyzed in addition to accuracy analysis. To achieve it, the standard deviation (STD) values were calculated using topocentric coordinates. The overall STDs of PPP and PPP-AR solutions are given for both satellite configurations in Table 3.

Table 3. The overall STDs

GPS		
	PPP	**PPP-AR**
North (mm)	1.62	1.54
East (mm)	2.12	1.21
Up (mm)	4.30	3.89
GPS+GLO		
	PPP	**PPP-AR**
North (mm)	1.56	1.50
East (mm)	2.02	1.20
Up (mm)	4.23	3.99

According to Table 3, the STD values for the horizontal components vary between 1.21 mm and 2.12 mm. Moreover, the STD values for the up component are between 3.89 mm and 4.30 mm. The error is defined as the difference of the PPP coordinates in relation to the assumed real values, which herein are the IGS weekly solutions. The error distributions of PPP and PPP-AR results are depicted in Figures 4–7.

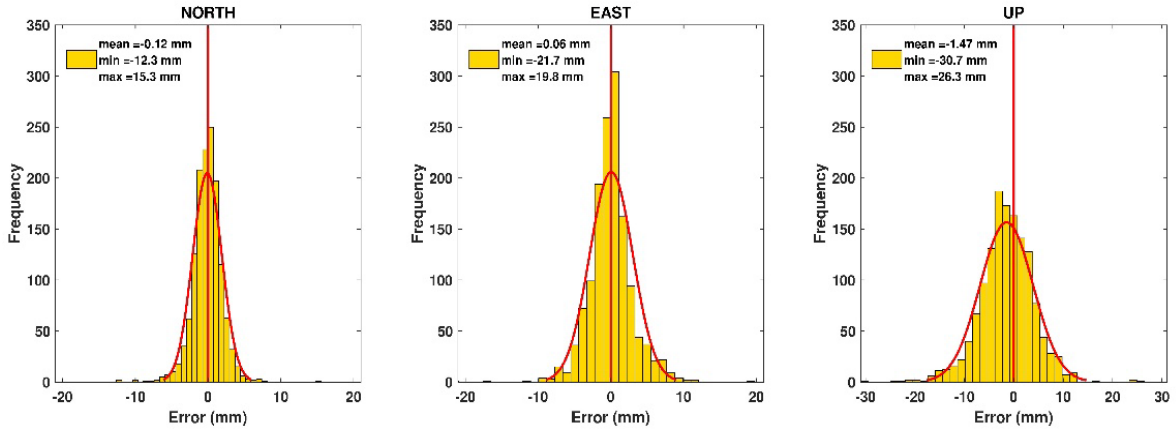

Figure 4. GPS PPP error distributions

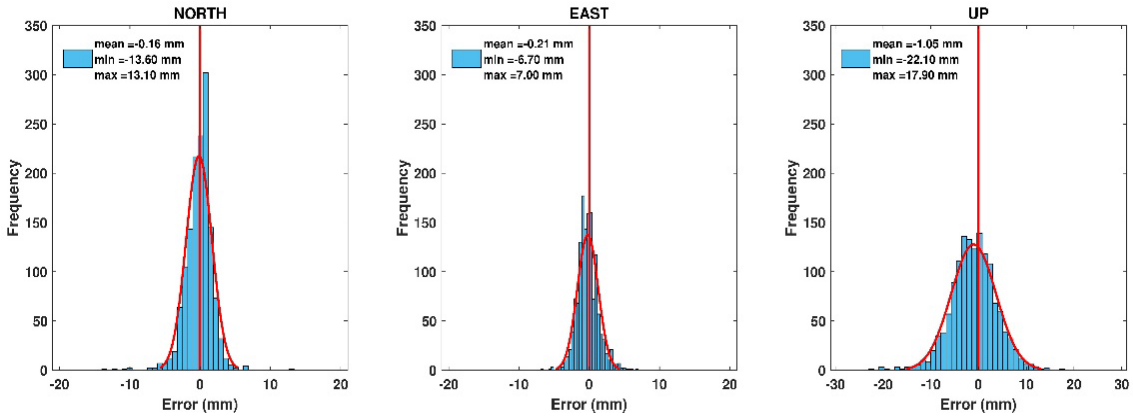

Figure 5. GPS PPP-AR error distributions

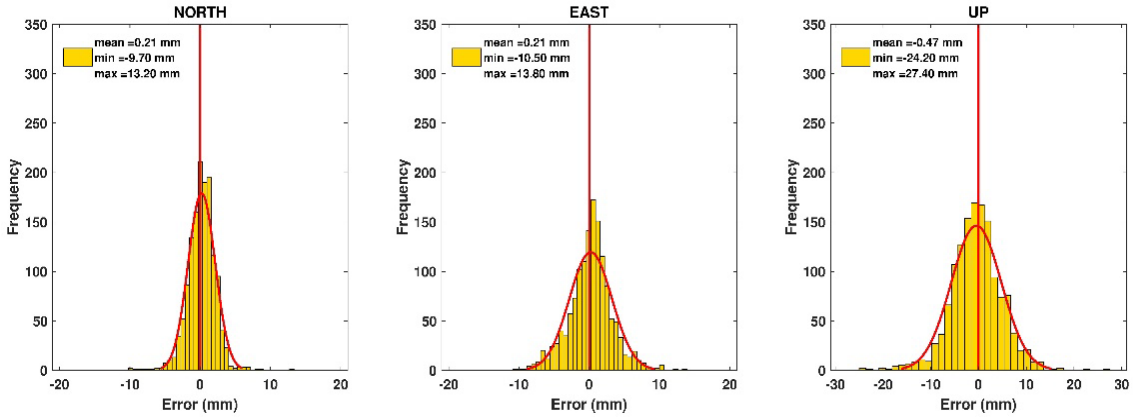

Figure 6. GPS + GLO PPP error distributions

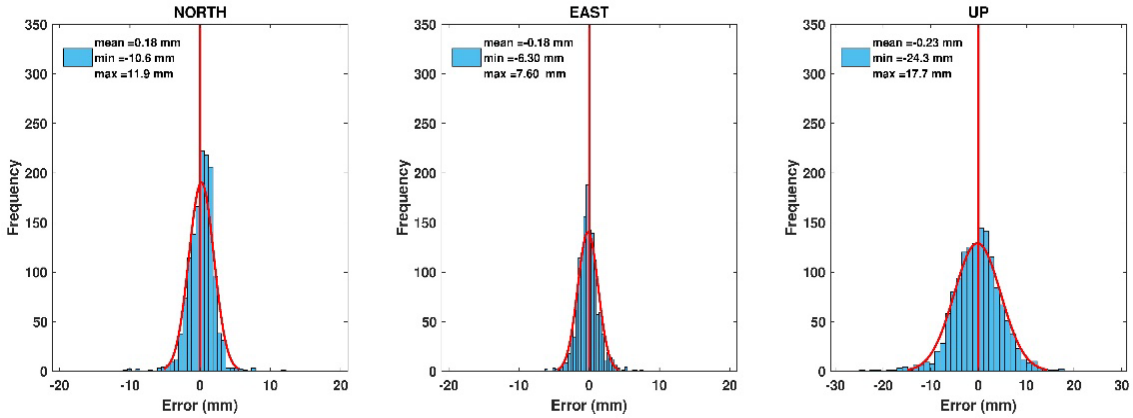

Figure 7. GPS + GLO PPP-AR error distributions

When the results in Figures 4–7 are analyzed, both PPP and PPP-AR solutions show a similar trend within the Gauss distribution. Thus, it is proved that there is no gross error in the solutions. As seen from Figures 4–7, the horizontal components are in the range of approximately −10.0/+10.0 mm, and the up component is in the range of approximately −20.0/+20.0 mm. The mean values of the horizontal components of GPS and GPS + GLO satellite configurations are better than 0.22 mm. However, the mean value of the up components of GPS PPP is −1.47 mm. For GPS solutions, the AR approach improved the PPP results by 0.42 mm to −1.05 mm in the up component. For the GPS + GLO satellite combination, the PPP-AR method improved the mean values of the up component by

0.24 mm. It is also clearly seen that PPP-AR results significantly shrink the error distribution range of the east component.

The convergence time is another topic related to positioning performance using the PPP method. In this study, the static PPP convergence times were calculated as the processing is based on forward filtering. For instance, the topocentric coordinate time series of PPP and PPP-AR solutions for the ARTU station on DOY-305 is given in Figure 8.

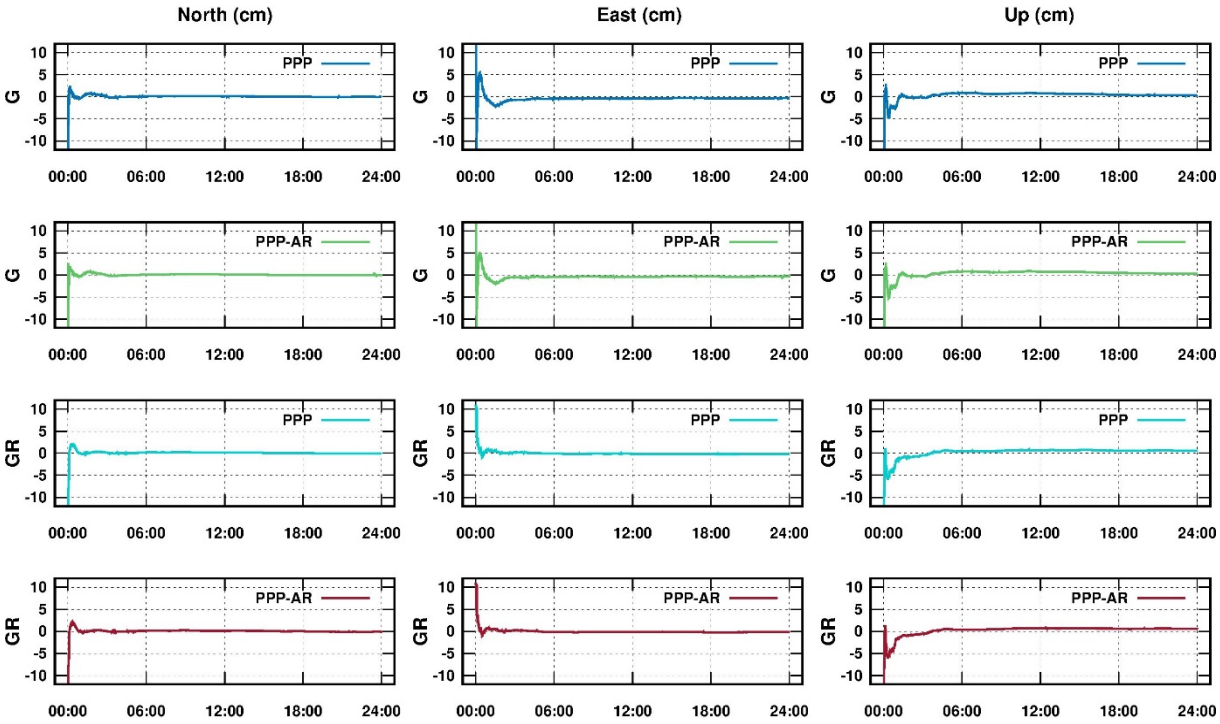

Figure 8. The coordinate time series of ARTU station on DOY-305

As illustrated in Figure 8, both GPS and GPS + GLO solutions were converged in a few epochs. The convergence times were calculated using a 10-cm threshold value and validated for 60 epochs (30 minutes). Thus, the mean convergence times were obtained for each station and processing option. The overall mean convergence times are given in Table 4.

Table 4. The overall mean convergence times

	GPS	**GPS+GLO**
PPP	21.4 min	13.1 min
PPP-AR	21.4 min	13.2 min

As depicted in Table 4, GPS-only PPP solutions converged to 10 cm before 21.5 minutes. However, the GLONASS satellites improved the convergence time by 8 minutes. Although AR is expected to improve convergence time, herein, it did not show any significant improvement on mean convergence times. For more in-depth analysis, the percentages of converged solutions were assessed for different time intervals. The distributions of converged ambiguity-float and ambiguity-fixed solutions considering different time intervals are shown in Figures 9 and 10.

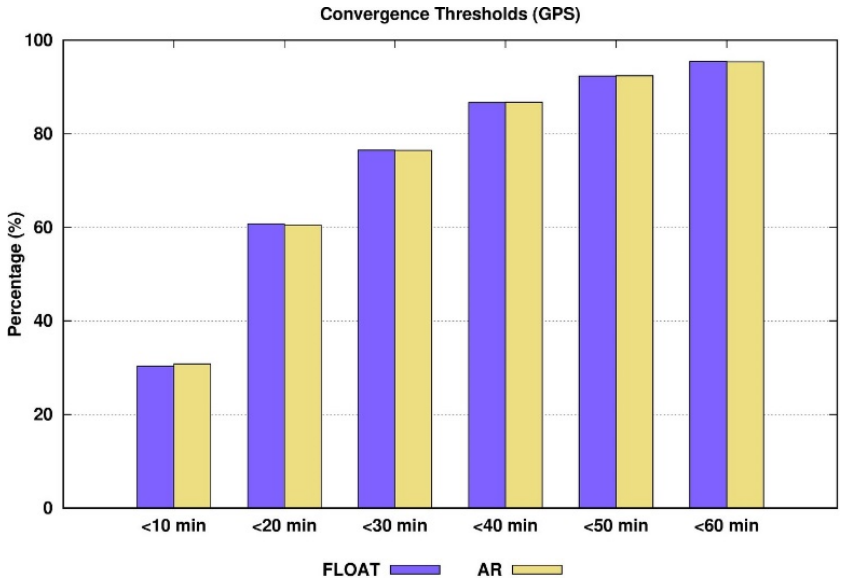

Figure 9. The distribution of converged GPS-only solutions

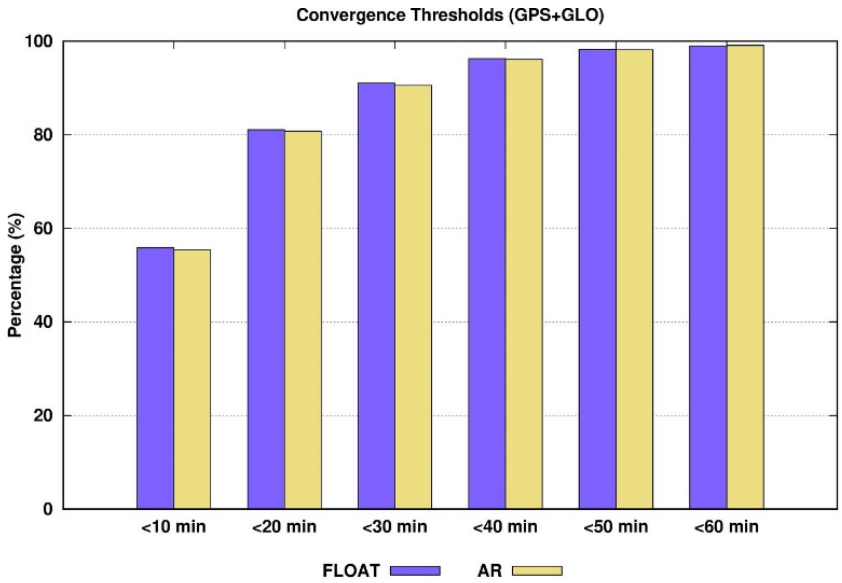

Figure 10. The distribution of converged GPS + GLO solutions

As seen in Figures 9 and 10, the number of converged solutions before 10 minutes is approximately 30% for GPS, while it is approximately 55% for GPS + GLO. Similarly, GPS + GLO gives better results for solutions in other time intervals. For PPP and PPP-AR solutions, no significant difference was seen in both GPS and GPS + GLO satellite configurations.

In addition to the positioning performance, the modernized CSRS-PPP was evaluated in terms of troposphere estimation. To achieve that, the ZTD values of the PPP and PPP-AR solutions were analyzed for both GPS and GPS + GLO satellite configurations. The ZTD values were compared to the state-of-art IGS final troposphere product. Moreover, it should be noted that the IGS final troposphere product comes in 5-minute time interval. Therefore, CSRS-PPP solutions were decimated to 5-minute epoch interval for comparison with their IGS counterparts. The differences between the CSRS-PPP ZTD values and the IGS ZTD values were calculated (ΔZTD). RMSE, STD, absolute maximum, and mean values of ΔZTD for PPP and PPP-AR solutions are presented in Table 5.

Table 5. The statistical results of ΔZTD values

GPS		
	PPP	**PPP-AR**
RMSE (mm)	7.3	5.8
STD (mm)	6.5	5.0
Abs. max (mm)	58.8	32.0
Mean (mm)	0.0	-0.1
GPS+GLO		
	PPP	**PPP-AR**
RMSE (mm)	7.1	6.0
STD (mm)	6.2	5.1
Abs. max (mm)	51.9	32.4
Mean (mm)	0.4	0.2

In Table 5, while an accuracy of about 7 mm is achieved with GPS PPP, the GPS PPP-AR model has improved the ZTD estimation by 1 mm. When the absolute maximum values are assessed, the AR approach has an undeniable contribution to PPP ZTD estimation. However, the GPS and GPS + GLO satellite configurations showed similar STD results.

5. CONCLUSIONS

In this study, the performance of modernized CSRS-PPP with AR was investigated from different aspects. The data of geographically distributed 47 IGS stations were processed before and after the software transition to PPP-AR. The new software provided an accuracy level of 1.7 mm, 1.4 mm, and 4.6 mm for the north, east, and up components only using GPS satellites. The results of this study showed that the AR feature improves the positioning accuracy at least by about 10%. For the east component, the improvement on using AR is >45% in both GPS-only and GPS–GLO cases. In addition to accuracy analysis, the static PPP convergence times were evaluated. Accordingly, while the GPS + GLO combination has an undeniable contribution over GPS-only PPP, AR does not improve the convergence time. Moreover, the performance of tropospheric delay estimation was analyzed by comparing CSRS-PPP ZTD solutions with IGS final ZTDs. The results indicate that the difference between the IGS final product and the modernized CSRS-PPP solution is <6 mm. It can be concluded that the new CSRS-PPP software can successfully be used for troposphere estimation. In conclusion, it is stated that the modernized CSRS-PPP service is a beneficial tool to achieve PPP-AR positioning and troposphere estimation.

Acknowledgements. The authors would like to thank Natural Resources Canada for providing the Canadian Spatial Reference System precise point positioning (CSRS-PPP) software. The authors also thank the International global navigation satellite system (GNSS) service for providing GNSS observation data and precise products.

REFERENCES

Alcay S., Gungor M. (2020). Investigation of ionospheric TEC anomalies caused by space weather conditions. *Astrophysics and Space Science*, 365(9), 1-15. https://doi.org/10.1007/s10509-020-03862-x

Alcay S., Inal C., Yigit C., Yetkin, M. (2012). Comparing GLONASS-only with GPS-only and hybrid positioning in various length of baselines. *Acta Geodaetica et Geophysica Hungarica*, 47(1), 1-12. https://doi.org/10.1556/AGeod.47.2012.1.1

Alcay S., Ogutcu S., Kalayci I., Yigit C.O. (2019). Displacement monitoring performance of relative positioning and Precise Point Positioning (PPP) methods using simulation apparatus, *Advances in Space Research*, 63, 5, 1697–1707. https://doi.org/10.1016/j.asr.2018.11.003

Alcay S., Turgut M. (2021). Evaluation of the positioning performance of multi-GNSS RT-PPP method, *Arabian Journal of Geosciences*, 14, 3, 155, https://doi.org/10.1007/s12517-021-06534-4.

Alcay S., Yigit C. O. (2017). Network based performance of GPS-only and combined GPS/GLONASS positioning under different sky view conditions. *Acta Geodaetica et Geophysica*, 52(3), 345-356. https://doi.org/10.1007/s40328-016-0173-5

Atiz O.F., Alcay S., Ogutcu S. (2020). Investigation of the Performance of Galileo only Precise Point Positioning, *International Conference on Engineering Technologies (ICENTE20)*, 19-21, November 2020, Konya, Turkey

Banville S., (2020). CSRS-PPP Version 3: Tutorial, https://webapp.geod.nrcan.gc.ca/geod/tools-outils/sample_doc_filesV3/NRCan%20CSRS-PPP-v3_Tutorial%20EN.pdf Accessed on 29.03.2021.

Banville S., Geng J., Loyer S., Schaer S., Springer T., Strasser S., (2020). On the interoperability of IGS products for precise point positioning with ambiguity resolution. *Journal of Geodesy*, 94(1), 10. https://doi.org/10.1007/s00190-019-01335-w

Banville S., Hassen E., Lamothe P., Farinaccio J., Donahue B., Mireault Y., Goudarzi M. A., Collins P., Ghoddousi-Fard R., Kamali O. (2021). Enabling ambiguity resolution in CSRS-PPP. *Navigation*, 68(2), 433– 451. https://doi.org/10.1002/navi.423

Bertiger W., Bar-Sever Y., Dorsey A., Haines B., Harvey N., Hemberger D., ... Willis P. (2020). GipsyX/RTGx, a new tool set for space geodetic operations and research. *Advances in Space Research*, 66(3), 469-489. https://doi.org/10.1016/j.asr.2020.04.015

Bulbul S., Bilgen B., Inal C. (2021). The performance assessment of Precise Point Positioning (PPP) under various observation conditions. *Measurement*, 171, 108780. https://doi.org/10.1016/j.measurement.2020.108780

Cai C., Gao Y. (2013). Modeling and assessment of combined GPS/GLONASS precise point positioning. *GPS Solutions*, 17(2), 223-236. https://doi.org/10.1007/s10291-012-0273-9

Cai C., Liu Z., Luo X. (2013). Single-frequency ionosphere-free precise point positioning using combined GPS and GLONASS observations. *The Journal of Navigation*, 66(3), 417-434. https://doi.org/10.1017/S0373463313000039

Collins P., Bisnath S., Lahaye F., Héroux, P. (2010). Undifferenced GPS ambiguity resolution using the decoupled clock model and ambiguity datum fixing. *Navigation*, 57(2), 123-135. https://doi.org/10.1002/j.2161-4296.2010.tb01772.x

Elsobeiey M., Al-Harbi S. (2016). Performance of real-time Precise Point Positioning using IGS real-time service. *GPS Solutions*, 20(3), 565-571. https://doi.org/10.1007/s10291-015-0467-z

Ge M., Gendt G., Rothacher M. A., Shi C., Liu J. (2008). Resolution of GPS carrier-phase ambiguities in precise point positioning (PPP) with daily observations. *Journal of Geodesy*, 82(7), 389-399. https://doi.org/10.1007/s00190-007-0187-4

Geng J., Chen X., Pan Y., Mao S., Li C., Zhou J., Zhang K. (2019). PRIDE PPP-AR: an open-source software for GPS PPP ambiguity resolution. *GPS Solutions*, 23(4), 1-10. https://doi.org/10.1007/s10291-019-0888-1

Goudarzi M. A., Banville S., 2018. Application of PPP with ambiguity resolution in earth surface deformation studies: a case study in eastern Canada. *Survey Review*, 50(363), 531-544. https://doi.org/10.1080/00396265.2017.1337951

Guo Q. (2015). Precision comparison and analysis of four online free PPP services in static positioning and tropospheric delay estimation. *GPS Solutions*, 19(4), 537-544. https://doi.org/10.1007/s10291-014-0413-5

Håkansson M., Jensen A. B., Horemuz M., Hedling G. (2017). Review of code and phase biases in multi-GNSS positioning. *GPS Solutions*, 21(3), 849-860. https://doi.org/10.1007/s10291-016-0572-7

Hu H., Gao J., Yao Y., 2014. Land deformation monitoring in mining area with PPP-AR. *International Journal of Mining Science and Technology*, 24(2), 207-212. https://doi.org/10.1016/j.ijmst.2014.01.011

Jokinen A., Feng S., Schuster W., Ochieng W., Hide C., Moore T., Hill C. (2013). GLONASS aided GPS ambiguity fixed precise point positioning. *The Journal of Navigation*, 66(3), 399-416. https://doi.org/10.1017/S0373463313000052

Katsigianni G., Loyer S., Perosanz F., (2019). PPP and PPP-AR Kinematic Post-Processed Performance of GPS-Only, Galileo-Only and Multi-GNSS. *Remote Sensing*, 11(21), 2477. https://doi.org/10.3390/rs11212477

Kouba J., Héroux P. (2001). Precise point positioning using IGS orbit and clock products. *GPS Solutions*, 5(2), 12-28. https://doi.org/10.1007/PL00012883

Krasuski K., C´wiklak J., Jafernik H. (2018). Aircraft positioning using PPP method in GLONASS system, *Aircraft Engineering and Aerospace Technology*, Vol. 90 No. 9, pp. 1413-1420. https://doi.org/10.1108/AEAT-06-2017-0147

Krzan G., Przestrzelski P. (2016). GPS/GLONASS precise point positioning with IGS real-time service products. *Acta Geodynamica et Geomaterialia*, 13(1), 69-81. https://doi.org/10.13168/AGG.2015.0047

Laurichesse D., Mercier F., Berthias J. P., Broca P., Cerri L. (2009). Integer ambiguity resolution on undifferenced GPS phase measurements and its application to PPP and satellite precise orbit determination. *Navigation*, 56(2), 135-149. https://doi.org/10.1002/j.2161-4296.2009.tb01750.x

Leick A., Rapoport L., Tatarnikov D. (2015). GPS Satellite Surveying. John Wiley & Sons.

Li X., Li X., Yuan Y., Zhang K., Zhang X., Wickert J., (2018). Multi-GNSS phase delay estimation and PPP ambiguity resolution: GPS, BDS, GLONASS, Galileo. *Journal of Geodesy*, 92(6), 579-608. https://doi.org/10.1007/s00190-017-1081-3

Melbourne W.G. (1985). The case for ranging in GPS-based geodetic systems. *1st International Symposium on Precise Point Positioning with GPS.* Rockville, Maryland.

Mendez Astudillo J., Lau L., Tang Y. T., Moore T. (2018). Analysing the zenith tropospheric delay estimates in on-line precise point positioning (PPP) services and PPP software packages. *Sensors*, 18(2), 580. https://doi.org/10.3390/s18020580

Ogutcu S., (2020a). Performance analysis of ambiguity resolution on PPP and relative positioning techniques: consideration of satellite geometry. *International Journal of Engineering and Geosciences*, 5(2), 73-93. https://doi.org/10.26833/ijeg.580027

Ogutcu S., (2020b). Assessing the contribution of Galileo to GPS+ GLONASS PPP: Towards full operational capability. *Measurement*, 151, 107143. https://doi.org/10.1016/j.measurement.2019.107143

Ogutcu S., Kalayci, I. (2016). Investigation of network-based RTK techniques: a case study in urban area. *Arabian Journal of Geosciences*, 9(3), 1-12. https://doi.org/10.1007/s12517-015-2262-0

Otsuka Y., Ogawa T., Saito A., Tsugawa T., Fukao S., Miyazaki S. (2002). A new technique for mapping of total electron content using GPS network in Japan. *Earth, Planets and Space*, 54(1), 63-70. https://doi.org/10.1007/s10291-006-0029-5

Pikridas C., Katsougiannopoulos S., Zinas N. (2014). A comparative study of zenith tropospheric delay and precipitable water vapor estimates using scientific GPS processing software and web based automated PPP service. *Acta Geodaetica et Geophysica*, 49(2), 177-188. https://doi.org/10.1007/s40328-014-0047-7

Shi J. (2012). Precise Point Positioning Integer Ambiguity Resolution with Decoupled Clocks (Unpublished doctoral thesis). University of Calgary, Calgary, AB. http://dx.doi.org/10.11575/PRISM/27397

Shi J., Gao Y. (2014). A comparison of three PPP integer ambiguity resolution methods. *GPS Solutions*, 18(4), 519-528. https://doi.org/10.1007/s10291-013-0348-2.

Subirana J. S., Zornoza J. J., Hernández-Pajares M. (2013). GNSS Data Processing. Volume 1: Fundamentals and Algorithms. *ESA Communications*, ESTEC, PO Box, 299, 2200.

Takasu T., Yasuda A. (2009, November). Development of the low-cost RTK-GPS receiver with an open source program package RTKLIB. *In International symposium on GPS/GNSS (Vol. 1)*. International Convention Center, Jeju, Korea.

Tegedor J., Liu X., Ørpen O., Treffers N., Goode M., Øvstedal O., (2015). Comparison between multi-constellation ambiguity-fixed PPP and RTK for maritime precise navigation. *Journal of Applied Geodesy*, 9(2), 73-80. https://doi.org/10.1515/jag-2014-0028

Tétreault P., Kouba J., Héroux P., Legree, P. (2005). CSRS-PPP: an internet service for GPS user access to the Canadian Spatial Reference Frame. *Geomatica*, 59(1), 17-28.

Wang G., Bao Y., Cuddus Y., Jia X., Serna J., Jing Q. (2015). A methodology to derive precise landslide displacement time series from continuous GPS observations in tectonically active and cold regions: a case study in Alaska. *Natural Hazards*, 77(3), 1939-1961. https://doi.org/10.1007/s11069-015-1684-z

Wu Q., Sun M., Zhou C., Zhang P. (2019). Precise point positioning using dual-frequency GNSS observations on smartphone. *Sensors*, 19(9), 2189. https://doi.org/10.3390/s19092189

Wübbena G. (1985) Software developments for geodetic positioning with GPS using TI-4100 code and carrier measurements. *1st International Symposium on Precise Point Positioning with GPS.* Rockville, Maryland.

Xiao G., Liu G., Ou J., Liu G., Wang S., Guo A. (2020). MG-APP: an open-source software for multi-GNSS precise point positioning and application analysis. *GPS Solutions,* 24(3), 1-13. https://doi.org/10.1007/s10291-020-00976-1

Yigit C.O, Gikas V., Alcay S., Ceylan A. (2014). Performance evaluation of short to long term GPS, GLONASS and GPS/GLONASS post-processed PPP, *Survey Review*, 46(3), 155-166. https://doi.org/10.1179/1752270613Y.0000000068

Zumberge J. F., Heflin M. B., Jefferson D. C., Watkins M. M., Webb F. H. (1997). Precise point positioning for the efficient and robust analysis of GPS data from large networks. *Journal of Geophysical Research: Solid Earth*, 102 (B3), 5005-5017. https://doi.org/10.1029/96JB03860

Received: *2021-04-27*

Reviewed: *2021-06-10 (undisclosed name) and 2021-06-21 (D. Próchniewicz)*

Accepted: *2021-06-30*